Supplementary Material to "Revisiting ignited-quenched transition and the non-Newtonian rheology of a sheared dilute gas-solid suspension"

Saikat Saha[1] and Meheboob Alam [1]†

[1]Engineering Mechanics Unit, Jawaharlal Nehru Centre for Advanced Scientific Research, Jakkur P.O., Bangalore 560064, India

(Received xx; revised xx; accepted xx)

Appendix A. Maximum entropy principle and the anisotropic Maxwellian distribution function

Appendix A is given in the main text of Saha & Alam (2017).

Appendix B. Source terms in quenched and ignited states

The integral expression for the source/production term in the second-moment balance is given by

$$\aleph = \int m\boldsymbol{CC}\left(\frac{\partial f}{\partial t}\right)_{coll} d\boldsymbol{C} = \frac{\sigma^2}{2}\int \Delta\Big(m\boldsymbol{CC}\Big) f(\boldsymbol{C}_1) f(\boldsymbol{C}_2)\,(\boldsymbol{g}\cdot\boldsymbol{k})\,d\boldsymbol{k}d\boldsymbol{C}_1 d\boldsymbol{C}_2. \quad \text{(B 1)}$$

The total change of the dyadic product $\boldsymbol{CC}$ in an inelastic collision can be written, using the collision rules

$$\boldsymbol{C}_1' = \boldsymbol{C}_1 - \frac{1}{2}(1+e)\,(\boldsymbol{g}\cdot\boldsymbol{k})\,\boldsymbol{k} \quad \text{and} \quad \boldsymbol{C}_2' = \boldsymbol{C}_2 + \frac{1}{2}(1+e)\,(\boldsymbol{g}\cdot\boldsymbol{k})\,\boldsymbol{k}, \quad \text{(B 2)}$$

and after some algebra, as

$$\Delta\Big(\boldsymbol{CC}\Big) = \frac{(1+e)}{2}\Big\{(1+e)\,(\boldsymbol{g}\cdot\boldsymbol{k})^2\,\boldsymbol{kk} - (\boldsymbol{g}\cdot\boldsymbol{k})\,\boldsymbol{kw} - (\boldsymbol{g}\cdot\boldsymbol{k})\,\boldsymbol{wk}\Big\}, \quad \text{(B 3)}$$

where $\boldsymbol{g} = \boldsymbol{c}_1 - \boldsymbol{c}_2$, and

$$\boldsymbol{w} = \boldsymbol{C}_1 - \boldsymbol{C}_2 = \boldsymbol{g} - (\boldsymbol{u}_1 - \boldsymbol{u}_2) = \boldsymbol{g} - \delta\boldsymbol{u} \quad \text{(B 4)}$$

is the relative 'fluctuation' velocity of two colliding particles and $\delta\boldsymbol{u} = (\boldsymbol{u}_1 - \boldsymbol{u}_2)$.

Upon substituting (B 3) and (B 4) into (B 1), we obtain

$$\aleph = \aleph_1 + \aleph_2 + \aleph_3, \quad \text{(B 5)}$$

where

$$\aleph_1 = \frac{m\sigma^2}{2}\frac{(1+e)}{2}\int \Big[(1+e)\,(\boldsymbol{w}\cdot\boldsymbol{k})\,\boldsymbol{kk} - (\boldsymbol{kw}+\boldsymbol{wk})\Big]\,(\boldsymbol{w}\cdot\boldsymbol{k})^2\,f_1 f_2 d\boldsymbol{k}d\boldsymbol{C}_1 d\boldsymbol{C}_2, \quad \text{(B 6)}$$

$$\aleph_2 = \frac{m\sigma^2}{2}\frac{(1+e)^2}{2}\int (\delta\boldsymbol{u}\cdot\boldsymbol{k})^3\,\boldsymbol{kk} f_1 f_2 d\boldsymbol{k}d\boldsymbol{C}_1 d\boldsymbol{C}_2, \quad \text{(B 7)}$$

† Email address for correspondence: meheboob@jncasr.ac.in

$$\aleph_3 = \frac{m\sigma^2}{2}\frac{(1+e)}{2}\int (\delta\boldsymbol{u}\cdot\boldsymbol{k})\Big[3(1+e)\big\{(\boldsymbol{w}\cdot\boldsymbol{k})+(\delta\boldsymbol{u}\cdot\boldsymbol{k})\big\}(\boldsymbol{w}\cdot\boldsymbol{k})\,\boldsymbol{k}\boldsymbol{k} - \big\{2(\boldsymbol{w}\cdot\boldsymbol{k})+(\delta\boldsymbol{u}\cdot\boldsymbol{k})\big\}(\boldsymbol{k}\boldsymbol{w}+\boldsymbol{w}\boldsymbol{k})\Big] f_1 f_2 d\boldsymbol{k} d\boldsymbol{C}_1 d\boldsymbol{C}_2. \tag{B 8}$$

In the quenched state, the particles are assumed to follow fluid velocity and hence $\boldsymbol{w}\approx 0$ and $\boldsymbol{g}=\delta\boldsymbol{u}$, yielding $\aleph_1 = 0 = \aleph_3$ and the final form of the source term

$$\aleph^{qs} \approx \aleph_2 = \frac{m\sigma^2}{2}\frac{(1+e)^2}{2}\int (\delta\boldsymbol{u}\cdot\boldsymbol{k})^3\,\boldsymbol{k}\boldsymbol{k} f_1 f_2 d\boldsymbol{k} d\boldsymbol{C}_1 d\boldsymbol{C}_2, \tag{B 9}$$

which is evaluated in (2.27) in the main text.

In the ignited state, $|\delta\boldsymbol{u}\cdot\boldsymbol{k}| \ll |\boldsymbol{w}|$ and $\boldsymbol{w}\approx\boldsymbol{g}$ and hence $\aleph_1$ dominates over $\aleph_2+\aleph_3$ and consequently we can write

$$\aleph^{\rm is} = \frac{m\sigma^2}{2}\frac{(1+e)}{2}\int \Big[(1+e)(\boldsymbol{g}\cdot\boldsymbol{k})\,\boldsymbol{k}\boldsymbol{k} - (\boldsymbol{k}\boldsymbol{g}+\boldsymbol{g}\boldsymbol{k})\Big](\boldsymbol{g}\cdot\boldsymbol{k})^2 f_1 f_2 d\boldsymbol{k} d\boldsymbol{C}_1 d\boldsymbol{C}_2. \tag{B 10}$$

Now for convenience of calculation using anisotropic Maxwellian we introduce a vector $\boldsymbol{j}$ that lies in the plane formed by $(\boldsymbol{g},\boldsymbol{k})$ and is perpendicular to the contact vector $\boldsymbol{k}$. Then the integral expression for $\aleph^{\rm is}$ modifies to

$$\aleph^{\rm is} = -\frac{m\sigma^2}{2}\frac{(1+e)}{2}\int \Big[(1-e)(\boldsymbol{g}\cdot\boldsymbol{k})\,\boldsymbol{k}\boldsymbol{k} + (\boldsymbol{k}\boldsymbol{j}+\boldsymbol{j}\boldsymbol{k})(\boldsymbol{g}\cdot\boldsymbol{j})\Big](\boldsymbol{g}\cdot\boldsymbol{k})^2 f_1 f_2 d\boldsymbol{k} d\boldsymbol{C}_1 d\boldsymbol{C}_2 \tag{B 11}$$

as in (2.24) in the main text.

Appendix C. Analysis in the ignited state for inelastic hard spheres

Appendix C is given in the main text of Saha & Alam (2017).

Appendix D. Coefficients a_i in equation (3.1)

Explicit expressions of the individual coefficients a_i appearing in equation (3.1) of the main text are given by:

$$a_{10} = 86416243200(3-e)^4(1-e)^3(1+e)^7\pi St^6\nu^7, \tag{D 1}$$

$$a_9 = 28805414400(3-e)^3(1-e)^2(1+e)^6(19-13e)\pi^{(3/2)}St^5\nu^6, \tag{D 2}$$

$$a_8 = 28576800(3-e)^2(1-e)(1+e)^5\pi^2St^4\nu^5\Big(252(197-278e+93e^2) + 5(1747-1438e+363e^2)St^2\Big), \tag{D 3}$$

$$a_7 = 3810240(3-e)(1+e)^4\sqrt{\pi}St^3\nu^4\Big(2100(1-e)(241-284e+79e^2)\pi^2 + 25(12607-19952e+10099e^2-1746e^3)\pi^2St^2 - 3456(3-e)^3(1-e)^2(1+e)^4St^3\nu^3\Big), \tag{D 4}$$

$$a_6 = 79380(1+e)^3\pi St^2\nu^3\Big(21000(1-e)(871-854e+199e^2)\pi^2 + 500(56617-78677e+35629e^2-5361e^3)\pi^2St^2 - 125(1691+539e-1223e^2+337e^3)\pi^2St^4$$

$$-27648(3-e)^3(1-e)(1+e)^4(29-23e)St^3\nu^3\Big), \tag{D 5}$$

$$a_5 = 18900(1+e)^2\pi^{(3/2)}St\nu^2\Big(441000(1-e)(23-11e)\pi^2$$
$$+10500(3437-3093e+688e^2)\pi^2St^2-875(477+442e-247e^2)\pi^2St^4$$
$$-580608(3-e)^2(1-e)(1+e)^4(11-7e)St^3\nu^3$$
$$-1152(3-e)^2(1+e)^4(991-934e+279e^2)St^5\nu^3\Big), \tag{D 6}$$

$$a_4 = 63(1+e)\nu\Big(165375000(1-e)\pi^4+656250(2437-1069e)\pi^4St^2$$
$$-109375(107+193e)\pi^4St^4-48384000(3-e)(1-e)(1+e)^4(37-19e)\pi^2St^3\nu^3$$
$$-288000(3-e)(1+e)^4(3917-3368e+843e^2)\pi^2St^5\nu^3$$
$$-3024000(3-e)^3(1+e)^4\pi^3St^6\nu^3+7962624(3-e)^4(1-e)(1+e)^8St^6\nu^6\Big), \tag{D 7}$$

$$a_3 = 2520\sqrt{\pi}St\Big(2296875\pi^4-504000(1-e)(1+e)^4(41-17e)\pi^2St\nu^3$$
$$-6000(1+e)^4(5617-4438e+933e^2)\pi^2St^3\nu^3-189000(3-e)^2(1+e)^4\pi^3St^4\nu^3$$
$$-1000(1+e)^4(1203-1002e+247e^2)\pi^2St^5\nu^3$$
$$+663552(3-e)^3(1-e)(1+e)^8St^4\nu^6\Big), \tag{D 8}$$

$$a_2 = -2400(1+e)^3\pi St\nu^2\Big(1323000(1-e)\pi^2+15750(383-151e)\pi^2St^2$$
$$+165375(3-e)\pi^3St^3+875(789-305e)\pi^2St^4$$
$$-870912(3-e)^2(1-e)(1+e)^4St^3\nu^3-1728(3-e)^2(1+e)^4(47-39e)St^5\nu^3\Big), \tag{D 9}$$

$$a_1 = -2000(1+e)^2\pi^{(3/2)}St^2\nu\Big(441000\pi^2+55125\pi^3St+98000\pi^2St^2$$
$$-580608(3-e)(1-e)(1+e)^4St\nu^3-3456(3-e)(1+e)^4(47-39e)St^3\nu^3\Big), \tag{D 10}$$

$$a_0 = 1440000(1+e)^5\pi^2St^2(4+St^2)\nu^3\Big(42(1-e)+(13-9e)St^2\Big). \tag{D 11}$$

Appendix E. Ordering analysis to determine three temperatures, and the limit of large St

We solve (3.1) analytically in the asymptotic limit $\nu \ll 1$, $St \gg 1$, and $St^3\nu \ll 1$ (Tsao & Koch 1995), and three feasible solutions have been found as described below. Note that the assumption of $St^3\nu \ll 1$ puts a restriction on the derived solutions to remain valid only at finite values of St for "inelastic" particles; however, the solution becomes exact (as in Appendix C) for the limiting case of a gas-solid suspension of elastically-colliding ($e = 1$) particles – the latter is due to the exact balance between the shear-work and the viscous dissipation as discussed in Appendix E.4.

E.1. *Temperature in the quenched state*

For $\xi \sim O(St^{3/2}\sqrt{\nu})$, the leading order term in (3.1) is $O(St^{\frac{11}{2}}\nu^{\frac{3}{2}})$ and consequently we have

$$a_3\xi^3 + a_1\xi = 0, \tag{E 1}$$

where

$$a_3 = 5788125000\pi^{\frac{9}{2}}St, \qquad a_1 = -196000000\pi^{\frac{7}{2}}(1+e)^2St^4\nu. \tag{E 2}$$

The solution at this level of approximation is

$$T_{qs} = \xi^2 = \frac{32(1+e)^2}{945\pi} St^3 \nu, \tag{E 3}$$

which corresponds to the temperature in the quenched state. Note that the quenched temperature increases with increasing both St and ν.

E.2. *Unstable temperature*

When $\xi \sim O(St^3\nu)^{-1}$, the highest-order term in (3.1) is $O(1/St^8\nu^3)$, and on neglecting terms smaller than this, we have at leading order

$$a_4\xi^4 + a_3\xi^3 = 0, \tag{E 4}$$

where

$$a_4 = -6890625(1+e)(107+193e)\pi^4 St^4\nu, \qquad a_3 = 5788125000\pi^{\frac{9}{2}} St. \tag{E 5}$$

Therefore, we have

$$\sqrt{T_{us}} = \xi = \frac{840\sqrt{\pi}}{(1+e)(107+193e)} \left(\frac{1}{St^3\nu}\right), \tag{E 6}$$

This is the temperature of an intermediate state which is unstable – note that T_{us} decreases with increasing St and ν.

E.3. *Temperature in the ignited state*

In the asymptotic limit of $\xi \sim O(St/\nu)$, the leading order term in (3.1) is $O(St^{12}/\nu^3)$ and consequently we have

$$a_7\xi^7 + a_6\xi^6 = 0, \tag{E 7}$$

where

$$\left.\begin{array}{rcl} a_7 &=& 95256000(3-e)(1+e)^4(12607-19952e+10099e^2-1746e^3)\pi^{\frac{5}{2}} St^5\nu^4 \\ a_6 &=& -9922500(1+e)^3(1691+539e-1223e^2+337e^3)\pi^3 St^6\nu^3. \end{array}\right\} \tag{E 8}$$

Therefore, the temperature at this order of approximation is

$$\sqrt{T_{is}} = \xi = \frac{5(1691+539e-1223e^2+337e^3)\sqrt{\pi}}{48(3-e)(1+e)(12607-19952e+10099e^2-1746e^3)} \left(\frac{St}{\nu}\right), \tag{E 9}$$

which corresponds to the temperature in the ignited state. While T_{is} increases with increasing St, it deceases with increasing the particle volume fraction ν.

E.4. *Scalings in the limit of large Stokes number*

To obtain the large shear-rate scaling (i.e. as $\dot{\gamma} \to \infty$) of temperature for "inelastic" particles suspended in a viscous gas, let us consider the energy equation (i.e. the trace of the second moment balance) under homogeneous shear

$$\mu\dot{\gamma}^2 = \mathcal{D}_{inelastic} + \mathcal{D}_{vis}, \tag{E 10}$$

where

$$\mathcal{D}_{vis} \sim T/\tau_v \sim \dot{\gamma} St^{-1} T \quad \text{and} \quad \mathcal{D}_{inelas} \sim (1-e^2)T^{3/2} \quad \text{with} \quad St = \dot{\gamma}\tau_v = \dot{\gamma}\left(\frac{m}{3\pi\mu_g\sigma}\right). \tag{E 11}$$

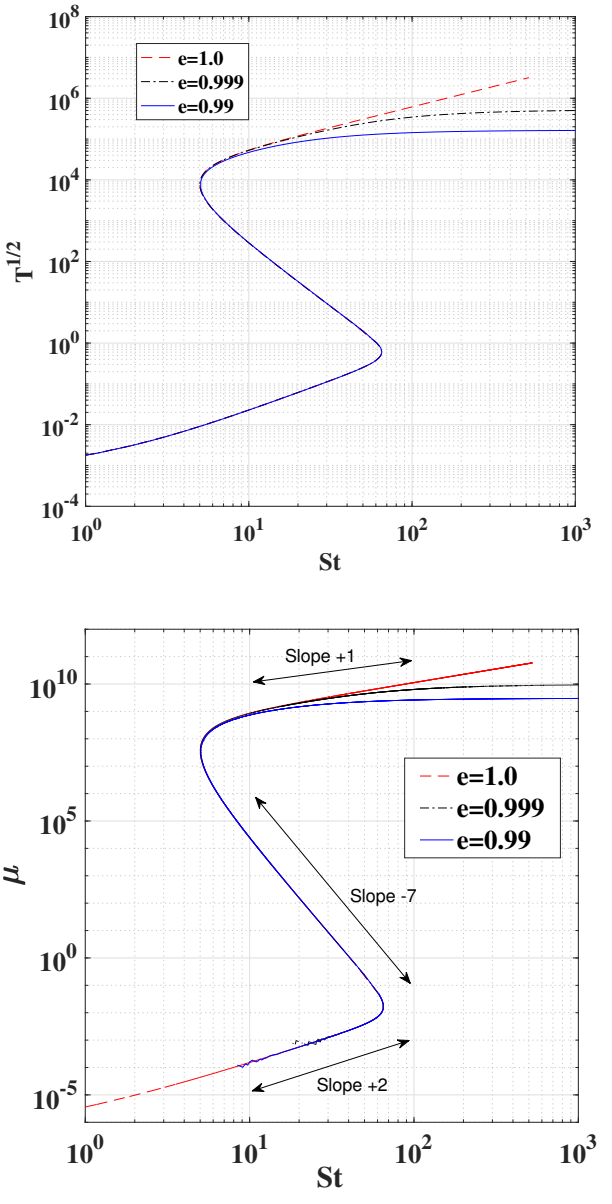

FIGURE E.1. (a) Variation of dimensionless temperature, $\sqrt{T} \equiv \sqrt{\widetilde{T}/(\dot{\gamma}\sigma/2)^2}$, with Stokes number $St = \dot{\gamma}\tau_v$ at a mean volume fraction of $\nu = 10^{-5}$. On the ignited-branch, the red-dashed line ($e = 1$) has a slope of 1 [and hence $\sqrt{T} \propto St \sim \dot{\gamma}$, $\Rightarrow \widetilde{T}(e = 1) \propto \dot{\gamma}^4$], whereas the "inelastic" curves ($e = 0.999, 0.99$) has nearly zero-slope [and hence $\widetilde{T}(e < 1) \propto \dot{\gamma}^2$] at $St > 300$. (b) Same as panel *a* but for dimensionless viscosity of the particle phase; see text for details.

Since $\mu \sim T^{1/2}$ and $\mathcal{D}_{vis} \to 0$ as $St = \dot{\gamma}\tau_v \to 0$, it immediately follows that the "dimensional" temperature (on ignited state) behaves like

$$\tilde{T}_{is} \sim \dot{\gamma}^2. \tag{E 12}$$

This quadratic scaling holds for an "inelastic" gas-solid suspension with $e \neq 1$ since the contribution of viscous dissipation vanishes in the limit of $St \to \infty$ (irrespective of the value of $e \neq 1$). This is evident in the insets of Fig. 2(b,c,d) where $\sqrt{\tilde{T}/\dot{\gamma}^2\sigma^2}$ is seen to approach a constant value.

For elastic particles ($e = 1$), however, the balance between shear work and viscous dissipation in (E 10) yields

$$\tilde{T}_{is} \sim \dot{\gamma}^4. \tag{E 13}$$

These scaling relations (E 12-E 13) were discussed by Sangani *et al.* (1996, see their equations 3.14 and 3.15). The 'change-in-scaling' from (E 12) to (E 13) is illustrated in figure E.1 which is obtained from the numerical solution of our Eqn. (3.1) in the main text. This figure also confirms the correct St-scaling of solutions in Eqn. (E6) and Eqn. (E3) for unstable ($\sqrt{T_{us}} \sim St^{-3}$) and quenched ($\sqrt{T_{qs}} \sim St^{3/2}$) states, respectively. In summary, the 'quartic' power-law scaling (of the ignited-branch temperature) for elastic particles changes to quadratic-scaling for inelastic particles as $St \to \infty$.

The above 'change-in-scaling' of temperature is directly tied to the shear-rate scaling of shear viscosity as illustrated in figure E.1(b):

$$\mu_{is} \propto St^{\alpha}, \quad \mu_{qs} \propto St^2 \quad \text{and} \quad \mu_{us} \propto St^{-7}, \tag{E 14}$$

where $\alpha = 1$ and 0 for $e = 1$ and $e < 1$, respectively; these exponents are marked over the respective double-arrow in figure E.1(b). In summary, while the ignited and quenched states are shear-thickening, the middle (unstable) branch is shear-thinning. The related issues are discussed in §4.2.1 of the main text.

Appendix F. Analytical determination of limit-points St_{c_1} and St_{c_2}

At the critical/limit points, two solution branches of equation (3.1) of the main text corresponding to two different states [(i) quenched (T_{qs}) and unstable (T_{us}) states and (ii) unstable (T_{us}) and ignited (T_{is}) states] meet and consequently we have saddle-node bifurcations from one stable state to another. Therefore, these limit points correspond to the double roots of (3.1) at which the following conditions must be satisfied:

$$\mathcal{G}(\xi_c) = 0 \quad \text{and} \quad \mathcal{G}'(\xi_c) = 0. \tag{F 1}$$

F.1. *Determining St_{c_1}: discontinuous transition from "ignited" to "quenched" states*

The critical Stokes number, St_{c_1}, for the transition from the ignited to quenched states corresponds to the limit point at which the temperatures corresponding to the ignited (T_{is}) and unstable (T_{us}) branches overlap with each other. Considering $\xi \sim O(\nu St)^{-1} \gg 1$, and retaining the highest-order terms, (3.1) reduces to

$$\mathcal{G} \approx a_7\xi^7 + a_6\xi^6 + a_5\xi^5 + a_4\xi^4 + a_3\xi^3 = 0 = a_7\xi^4 + a_6\xi^3 + a_5\xi^2 + a_4\xi + a_3, \tag{F 2}$$

$$\text{and} \quad 4a_7\xi^3 + 3a_6\xi^2 + 2a_5\xi + a_4 = 0, \tag{F 3}$$

where

$$\left.\begin{aligned} a_7 &= 95256000(3-e)(1+e)^4(12607-19952e+10099e^2-1746e^3)\pi^{\frac{5}{2}}St^5\nu^4 \\ a_6 &= 9922500(1+e)^3\pi^3St^4\Big(4(56617-78677e+35629e^2-5361e^3) \\ &\qquad -(1691+539e-1223e^2+337e^3)St^2\Big)\nu^3 \\ a_5 &= 16537500(1+e)^2\pi^{\frac{7}{2}}St^3\Big(12(3437-3093e+688e^2) \\ &\qquad -(477+442e-247e^2)St^2\Big)\nu^2 \\ a_4 &= 6890625(1+e)\pi^4St^2(6(2437-1069e)-(107+193e)St^2)\nu \\ a_3 &= 5788125000\pi^{\frac{9}{2}}St. \end{aligned}\right\} \tag{F 4}$$

Using the condition of equal roots of a fourth-degree polynomial (F 2), we obtain an expression for the critical Stokes number for the "ignited-to-unstable" transition:

$$St_{c_1} \approx 9.9 - 4.91e. \tag{F 5}$$

While decreasing the Stokes number along the ignited-state branch (see figure 2), the system jumps from the ignited to the quenched state at $St < St_{c_1}$ for all $\nu < \nu^l_{us}$ [equation (3.9) in the main text of Saha & Alam (2017)]. Therefore, (F 5) represents the minimum/critical Stokes number below which (3.1) admits the unique "quenched" state solution.

F.2. *Determining St_{c_2}: discontinuous transition from "quenched" to "ignited" state*

The limit point corresponding to the overlap of the quenched and unstable branches of the system is denoted by the Stokes number St_{c_2} at which the temperatures associated with the quenched (T_{qs}) and unstable (T_{us}) states coincide – above this critical value of Stokes number the quenched state ceases to exist. Mathematically, St_{c_2} is the point of the double root $T_{qs} = T_{us}$ of (3.1) above which there exists only one feasible solution T_{is} (corresponding to the ignited state) and the system jumps from the quenched state into the ignited state At this order of approximation $\xi \sim O(1)$ and the highest order terms are of the orders of νSt^4 and St. Therefore on neglecting the terms of $O(St^4\nu^2)$ and using the statement of $T_{qs} = T_{us}$, we have from (3.1)

$$\mathcal{G}(\xi_c) \approx a_4\xi^4 + a_3\xi^3 + a_1\xi = 0 = a_4\xi^3 + a_3\xi^2 + a_1, \tag{F 6}$$

$$\text{and} \quad \mathcal{G}'(\xi_c) \approx 3a_4\xi^2 + 2a_3\xi = 0, \tag{F 7}$$

where

$$\left.\begin{aligned} a_4 &= -6890625(1+e)(107+193e)\pi^4St^4\nu \\ a_3 &= 5788125000\pi^{\frac{9}{2}}St \\ a_1 &= -196000000(1+e)^2\pi^{\frac{7}{2}}St^4\nu. \end{aligned}\right\} \tag{F 8}$$

It follows from (F 7) that

$$\xi_c = \frac{-2a_3}{3a_4} = \frac{560\sqrt{\pi}}{(1+e)(170+193e)St^3\nu}. \tag{F 9}$$

On substituting (F 9) into (F 6) we obtain the *critical-surface*

$$St^3_{c_2}\nu_c = \left(\frac{3087000\pi^2}{(1+e)^4(107+193e)^2}\right)^{\frac{1}{3}}, \tag{F 10}$$

above which only the ignited state exists.

Appendix G. Suspension viscosity and connection with other works

G.1. *Suspension viscosity in quenched state*

The second-moment balance equation for the quenched state of the particle phase is given by

$$\frac{P_{\delta\beta}}{\rho(\dot{\gamma}\sigma/2)^2}\frac{1}{\dot{\gamma}}u_{\alpha,\delta}+\frac{P_{\delta\alpha}}{\rho(\dot{\gamma}\sigma/2)^2}\frac{1}{\dot{\gamma}}u_{\beta,\delta}+\frac{2}{St}\frac{P_{\alpha\beta}}{\rho(\dot{\gamma}\sigma/2)^2}=\frac{\aleph^{qs}_{\alpha\beta}}{\rho\dot{\gamma}^3(\sigma/2)^2}, \tag{G 1}$$

where the expression for the source-term $\aleph^{qs}_{\alpha\beta}$ can be found in (2.27) in the main text. The solution to the above equation for granular temperature is

$$T^*=\frac{T}{(\dot{\gamma}\sigma/2)^2}=\frac{32(1+e)^2\nu St^3}{945\pi}\left(1+\frac{9\pi}{16St}+\frac{9}{2St^2}\right). \tag{G 2}$$

It is straightforward to verify that the dimensionless shear stress is given by

$$P^*_{xy}\equiv\frac{P_{xy}}{\rho(\dot{\gamma}\sigma/2)^2}=-\eta\cos(2\phi)T^*=-\frac{2(1+e)^2\nu St}{35}\left(1+\frac{16}{9\pi}St\right). \tag{G 3}$$

For homogeneous shear, we have $P_{xy}=-\mu_{qs}\dot{\gamma}$ and hence the expression for (dimensional) shear viscosity in the quenched state is

$$\mu_{qs}=\frac{1}{70}\rho_p\nu^2\left(\frac{St^2}{\tau_v}\right)(1+e)^2\sigma^2\left(1+\frac{16}{9\pi}St\right). \tag{G 4}$$

Inserting the expression for relaxation time

$$\tau_v=\frac{m}{3\pi\mu_g\sigma}, \tag{G 5}$$

into (G 4) leads to the following expression

$$\mu_{\rm qs}=\mu_g\frac{(1+e)^2}{2}\nu^2\left(\frac{32St}{35\pi}+\frac{18}{35}\right)St^2 \tag{G 6}$$

for the 'quenched-state' viscosity of the 'particle-phase' at finite Stokes number ($St>0$). This expression (G 6) differs from that of Tsao & Koch (1995) by a numerical factor of 2 for a suspension of elastic ($e=1$) particles.

Adding (G 6) to the well-known Einstein-Batchelor formula (Batchelor & Green 1972; Batchelor 1977) of viscosity for a dilute Stokesian suspension

$$\mu_{eff}(St=0)=\mu_g(1+2.5\nu+6.2\nu^2)+O(\nu^3), \tag{G 7}$$

we arrive at the "suspension"/"effective" viscosity of a dilute 'granular' ($e\leqslant 1$) suspension at finite Stokes number:

$$\frac{\mu_{sus}}{\mu_g}=1+2.5\nu+\nu^2\left[6.2+St^2\frac{(1+e)^2}{2}\left(\frac{32St}{35\pi}+\frac{18}{35}\right)\right]+O(\nu^3St^3). \tag{G 8}$$

It is clear that finite St-correction appears at $O(\nu^2)$, with a numerical factor depending on the restitution coefficient.

G.2. *Connection with other works and DST*

We became aware of a recent work that uses gas kinetic theory (Hayakawa & Takada 2016; Hayakawa, Takada & Garzo 2017) in the context of a "thermalized" granular gas. On the ignited branch, the scaling of granular temperature (and also that of shear viscosity) with shear rate is found to be identical (quartic- and quadratic dependence

with shear rate for elastic and inelastic particles, respectively) in both works. It must be noted that while Hayakawa & Takada developed an effective "one-fluid" theory for a suspension, yielding an expression for the suspension viscosity, the present work (as well as Tsao & Koch (1995)) deals with a "mixture" theory having separate balance equations for the particle and gas phases. Therefore, the effective viscosity of a dilute suspension in the quenched state under the present formalism can be obtained as (G 8) as discussed in Appendix G.1. In the collisional regime of rapid granular flows, it is known that $\mu_p \gg \mu_g$ (i.e. the gas-phase has negligible contributions to the collisional viscosity of particles) and therefore $\mu_{sus} \approx \mu_p$ (where $\mu_p = \mu_{is}$ is the viscosity of the particle phase in the ignited state), thereby tying one-fluid and two-fluid formalisms in the large Stokes-number regime of a gas-solid suspension (and hence on the ignited branch). They also introduced a bath temperature ($T_{ex} > 0$) for the suspension that yields a Newtonian branch for viscosity at small shear rates – this could be an analog of our suspension viscosity (G 8) in the quenched state. In fact, their 'finite' bath temperature corresponds to the present zero-temperature state (see Appendix C) below a minimum Stokes number.

The finding of Hayakawa & Takada (2016) on discontinuous shear thickening (DST) as a "saddle-node" bifurcation appears similar to the present findings; they carried out one-dimensional stability analyses of three solutions which confirmed that the shear-thinning branch is indeed unstable. However, the connection of the present system of a dilute "gas-solid" suspension (with the gas-phase undergoing Stokes flow) with a thermalized granular gas (in which the Brownian forces influence the velocity distribution) remains unclear, especially in the small shear-rate regime where the ignited-quenched transition occurs. These issues can be reconciled in future.

In the area of liquid-solid suspensions (Brady & Bossis 1988; Boyer, Pouliquen & Guazzelli 2011), the shear-thickening and its discontinuous analog are well-known starting from the seminal experiments of Hoffman (1972). There have been a renewed research activity to understand the origin of DST in the "dense" regime of colloidal and non-colloidal suspensions as well as in dense granular media (Brown & Jaeger 2014; Denn & Morris 2014). Extending the present theoretical formalism to the dense regime of suspensions, by incorporating frictional interactions and related physics (Seto et al. 2013; Fernandez et al. 2013; Wyart & Cates 2014; Clavaud et al. 2017), would be an interesting future work.

Appendix H. Grad moment expansion (GME) for inelastic gas-solid suspension

Appendix H is given in the main text of Saha & Alam (2017).

Appendix I. Burnett-order solution of Sela and Goldhirsch (1998)

Sela & Goldhirsch (1998) solved the inelastic Boltzmann equation perturbatively via a Chapman-Enskog-like expansion around the Maxwellian distribution function. They carried out a "double-expansion" in terms of two small parameters: (i) the Knudsen number (Kn) and (ii) the inelasticity ($\epsilon = (1 - e^2)^{1/2}$); while the former is a measure of the gradients of hydrodynamic fields, the latter is a measure of the degree of inelastic dissipation. Since in the double-limit of $Kn \to 0$ and $\epsilon \to 0$, the sheared granular gas approaches the rest state of a molecular gas, the leading term of the Chapman-Enskog expansion is still the Maxwellian distribution function. The details can be found in the original article, and here we write down their Burnett-order expression for the stress

tensor:

$$P_{\alpha\beta} = \rho T\delta_{\alpha\beta} - 2\tilde{\mu}\rho l(3T)^{1/2}\overline{\frac{\partial u_\alpha}{\partial x_\beta}} + \tilde{\omega}_1\rho l^2(\boldsymbol{\nabla}\cdot\boldsymbol{u})\overline{\frac{\partial u_\alpha}{\partial x_\beta}}$$
$$-\tilde{\omega}_2\rho l^2\left(\overline{\frac{\partial}{\partial x_\alpha}\left(\frac{1}{\rho}\frac{\partial(\rho T)}{\partial x_\beta}\right)} + \overline{\frac{\partial u_\alpha}{\partial x_\delta}\frac{\partial u_\delta}{\partial x_\beta}} + 2\overline{\overline{\frac{\partial u_\alpha}{\partial x_\delta}}\frac{\partial u_\delta}{\partial x_\beta}}\right) + 3\tilde{\omega}_3\rho l^2\overline{\frac{\partial^2 T}{\partial x_\alpha\partial x_\beta}}$$
$$+3\tilde{\omega}_4\frac{l^2}{T}\overline{\frac{\partial(\rho T)}{\partial x_\alpha}\frac{\partial T}{\partial x_\beta}} + 3\tilde{\omega}_5\frac{\rho l^2}{T}\overline{\frac{\partial T}{\partial x_\alpha}\frac{\partial T}{\partial x_\beta}} + \tilde{\omega}_6\rho l^2\overline{\overline{\frac{\partial u_\alpha}{\partial x_\delta}}\ \overline{\frac{\partial u_\delta}{\partial x_\beta}}}, \tag{I 1}$$

where $l = 1/\pi n\sigma^2$ is the mean free-path, $\tilde{\omega}_i$'s are constants, and an over-bar on any tensorial quantity denotes its traceless part.

For the uniform shear flow $\boldsymbol{u} = (\dot{\gamma}y, 0, 0)$, the density ρ, the shear rate $\dot{\gamma}$ and the granular temperature T remain constants, and consequently the non-zero components of the stress tensor follow from (I 1):

$$\left.\begin{array}{lcl} P_{xx} &=& \rho T + \frac{1}{12}(\tilde{\omega_6} + 4\tilde{\omega_2})\rho l^2\dot{\gamma}^2 \\ P_{yy} &=& \rho T + \frac{1}{12}(\tilde{\omega_6} - 8\tilde{\omega_2})\rho l^2\dot{\gamma}^2 \\ P_{zz} &=& \rho T - \frac{1}{6}(\tilde{\omega_6} - 2\tilde{\omega_2})\rho l^2\dot{\gamma}^2 \\ P_{xy} &=& -\tilde{\mu}\rho l\dot{\gamma}\sqrt{3T}. \end{array}\right\} \tag{I 2}$$

By substituting the above stress tensor and the related expression for the collisional dissipation rate (not shown) into the granular energy balance equation, we obtain an expression for the granular temperature:

$$\frac{T}{l^2\dot{\gamma}^2} = \frac{4\tilde{\mu} - (1-e^2)\tilde{\rho_1}}{6\tilde{\delta}}, \tag{I 3}$$

where

$$\tilde{\mu} \approx 0.3249 + 0.0576(1-e^2), \quad \text{and} \quad \tilde{\delta} \approx \sqrt{\frac{16}{27\pi}}(1-e^2) - 0.0112(1-e^2)^2, \tag{I 4}$$

with $\tilde{\rho_1} = 0.1338$, $\tilde{\omega_2} = 0.6422$ and $\tilde{\omega_6} = 2.3510$. The expressions for the first and second normal stress differences follow directly from (I 2-I 3):

$$\left.\begin{array}{lcl} \mathcal{N}_1 &=& \frac{P_{xx}-P_{yy}}{p} = \frac{6\tilde{\omega_2}\tilde{\delta}}{4\tilde{\mu}-(1-e^2)\tilde{\rho_1}} \\ \mathcal{N}_2 &=& \frac{P_{yy}-P_{zz}}{p} = \frac{3(\tilde{\omega_6}-4\tilde{\omega_2})\tilde{\delta}}{2(4\tilde{\mu}-(1-e^2)\tilde{\rho_1})}, \end{array}\right\} \tag{I 5}$$

where $p = \rho T$ is the pressure. Expressions (I 5) are written in simplified forms in equation (5.5) in the main text as functions of the restitution coefficient.

REFERENCES

Batchelor, G. K. & Green, J. T. 1972 The determination of the bulk stress in a suspension of spherical particles to order c^2. *J. Fluid Mech.* **56**, 401-427.

Batchelor, G. K. 1977 Effect of Brownian motion on the bulk stress in a suspension of spherical particles. *J. Fluid Mech.* **83**, 97-117.

Boyer, F., Pouliquen, O. & Guazzelli, E. 2011 Dense suspensions in rotating-rod flows: normal stresses and particle migration. *J. Fluid Mech.* **686**, 5-25.

Brady, J. F. & Bossis, G. 1988 Stokesian dynamics. *Ann. Rev. Fluid Mech.* **20**, 111-157.

Brown, E. & Jaeger, H. M. 2014 Shear thickening in concentrated suspensions. *Rep. Prog. Phys.*, **77**, 046602.

Clavaud, C., Berut, A., Metzger, B. & Forterre, Y. 2017 Revealibg the frictional transition in shear-thickening suspensions. *Proc. Nat. Acad. Sci.* **114**, 5147-5152.

Denn, M. M. & Morris, J. F. 2014 Rheology of non-Brownian suspensions. *Annu. Rev. Chem. Biomol. Eng.*, **5**, 203-228.

Fernandez, N., Mani, R., Rinaldi, D., Kadau, D., Mosquet, M., Lombois-Burger, H., Cayer-Barrioz, J., Herrmann, H. J., Spencer, N. D. & Isa, L. 2013 Microscopic mechanism for shear thickening of non-Brownian suspensions. *Phys. Rev. Lett.* **111**, 108301.

Hayakawa, H. & Takada, S. 2016 Kinetic theory of shear-thickening for a dilute gas-solid suspension. arXiv:1611.07295

Hayakawa, H., Takada, S. & Garzo, V. 2017 Kinetic theory of shear-thickening for a moderately-dense gas-solid suspension– from discontinuous thickening to continuous thickeing. *Phys. Rev. E* (arxiv:1707.09694).

Hoffman, R. L. 1972 Discontinuous and dilatant viscosity behaviour in concentrated suspensions. *Trans. Soc. Rheol.* **16**, 155.

Saha, S. & Alam, M. 2017 Revisiting ignited-quenched transition and the non-Newtonian rheology of a sheared dilute gas-solid suspension. *J. Fluid Mech.* **83?** (December 25), 1-37 (In press)

Sangani, A. S., Mo, G., Tsao, H-K. & Koch, D. L. 1996 Simple shear flows of dense gas-solid suspensions at finite stokes numbers. *J. Fluid Mech.* **313**, 309-341.

Sela, N. & Goldhirsch, I. 1998 Hydrodynamic equations for rapid flows of smooth inelastic spheres, to Burnett order. *J. Fluid Mech.* **361**, 41-74.

Seto, R., Mari, R., Morris, J. F. & Denn, M. 2013 Discontinuous shear thickening of frictional hard-sphere suspensions. *Phys. Rev. Lett.* **111**, 218301.

Tsao, H-K. & Koch, D. L. 1995 Simple shear flows of dilute gas-solid suspensions. *J. Fluid Mech.* **296**, 211-246.

Wyart, M. & Cates, M. 2014 A model for discontinuous shear-thickening in dense non-Brownian suspensions. *Phys. Rev. Lett.*, **1**12, 098302.